

PACS numbers: 41.75.Fr; 41.75.Jv; 42.62. –b; 07.78.+s
DOI: 10.1070/QE2009v039n11ABEH014103

Electron beam deflection, focusing, and collimation by a femtosecond laser lens

V.G. Minogin

***Abstract*. This work examines spatial separation of femtosecond electron bunches using the ponderomotive potential created by femtosecond laser pulses. It is shown that ponderomotive optical potentials are capable of effectively deflecting, focusing, and collimating narrow femtosecond electron bunches.**

Keywords: *electron beam, femtosecond pulses, focusing, deflection, collimation.*

1. Introduction

The generation of femtosecond electron bunches is of considerable interest because they can be used to probe fast physicochemical processes. Basically, all techniques for producing ultrashort electron bunches can be divided into two approaches. In one approach, ultrashort electron bunches are generated directly in the process of photoelectron production [1 – 6]. In the other, this is achieved via spatial separation of ultrashort electron pulses from pregenerated electron bunches [7 – 10].

In recent years, most effort has been concentrated on the former approach, which takes advantage of evanescent fields at dielectric – vacuum interfaces. This approach, however, has inherent limitations: the incident laser beam intensity must not exceed the damage threshold of the dielectric [11, 12]. The latter approach, essentially free of such limitations, is of considerable interest because it offers greater possibilities for controlling the parameters of electron bunches. In this context, it is reasonable to raise the question of how the ponderomotive potentials created by femtosecond pulses directly act on electron beams with the aim of generating femtosecond electron bunches. Hebeisen et al. [9] have recently demonstrated deflection of a 55-keV electron beam by laser pulses with an intensity of 10^{17} W cm^{-2} and achieved an electron pulse duration of ~ 400 fs. At the same time, their results show that the use of high-energy electron beams leads to a rather weak effect of the ponderomotive potential on transverse electron velocities because of the short electron transit time in the interaction zone.

V.G. Minogin Institute for Spectroscopy, Russian Academy of Sciences, Fizicheskaya ul. 5, 142190 Troitsk, Moscow region, Russia; e-mail: minogin@isan.troitsk.ru

Received 13 March 2009; revision received 29 July 2009
Kvantovaya Elektronika **39** (11) 1095 – 1098 (2009)
Translated by O.M. Tsarev

This work examines the possibility of using the ponderomotive optical potential for effective spatial separation of femtosecond electron bunches from narrow low-energy electron beams. We analyse the effect of the ponderomotive optical potential created by a femtosecond optical pulse on the propagation of nonrelativistic electron bunches and show that the ponderomotive potential can deflect, focus, and collimate femtosecond electron bunches. The below examples of electron propagation in the field of femtosecond laser pulses confirm the feasibility of designing components of femtosecond electron beam optics based on femtosecond laser radiation with an intensity of $\sim 10^{14}$ to 10^{15} W cm^{-2}.

2. Electron beam deflection by a Gaussian laser beam

The simplest geometry in which a pulsed ponderomotive potential may effectively deflect a nonrelativistic electron beam is off-axis irradiation of the electron beam with femtosecond laser pulses. Consider a simple configuration in which an electron beam with angular divergence 2θ, issuing from a region of cross-sectional size δd at the origin and propagating along the x axis, is exposed to a focused beam of pulsed laser radiation propagating along the z axis. The laser beam axis is shifted from the origin by a distance l along the x axis and by a distance d along the y axis (Fig. 1a).

The electron beam is taken to have a broad initial temporal intensity profile, of width $2\tau_e$, with the pulse maximum at the origin at time $t = 0$ (Fig. 2). The laser beam has Gaussian spatial and temporal profiles with 1/e widths of $2w$ and $2\tau_{las}$, respectively:

$$I(x, y, t) = I_0 u(x, y, t), \tag{1}$$

$$u(x, y, t) = \exp\left[-\frac{(x-l)^2 + (y-d)^2}{w^2}\right] \times \exp\left[-\left(\frac{t-t_0}{\tau_{las}}\right)^2\right], \tag{2}$$

where I_0 is the peak intensity of the laser pulse and t_0 is the time delay between the laser pulse maximum and the initial electron pulse maximum, i.e., the delay relative to the instant at which the electron pulse maximum was at the origin (Fig. 2).

In what follows, we consider laser beam intensities at which the ponderomotive potential can be treated in the nonrelativistic approximation. In this approximation, the ponderomotive potential is given by

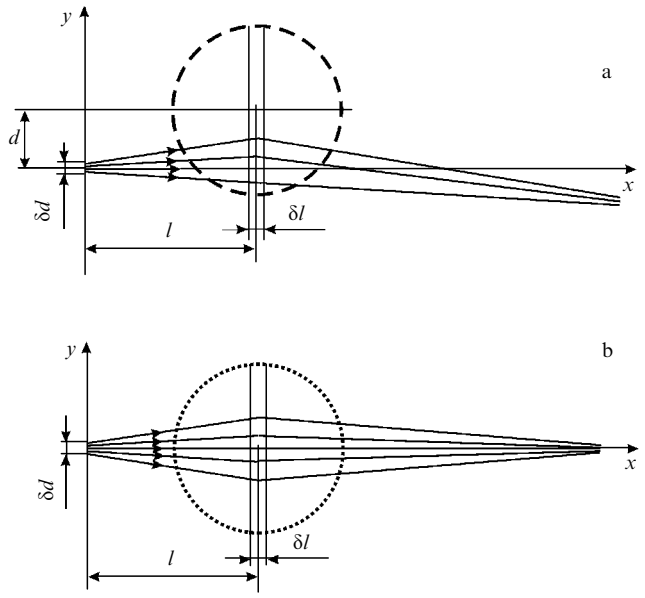

Figure 1. Schematics of (a) an electron beam deflector utilising a pulsed Gaussian laser beam, and (b) an electron beam focusing or collimating lens utilising a pulsed hollow laser beam. The dashed line shows the cross section of the Gaussian beam, and the dotted line shows the cross section of the hollow beam. l is the distance travelled by an electron during a laser pulse.

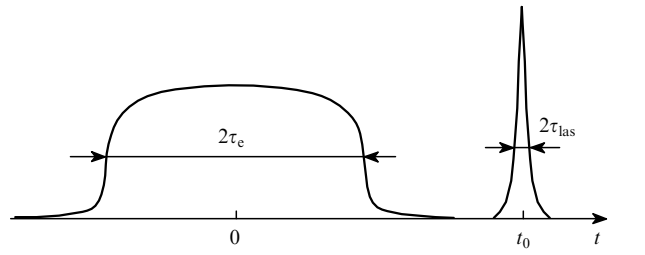

Figure 2. Unaffected electron pulse of duration $2\tau_e$ and laser pulse of duration $2\tau_{las}$.

$$U(x,y,t) = U_0 u(x,y,t), \tag{3}$$

where

$$U_0 = \frac{e^2\lambda^2 I_0}{2\pi m c^3} \tag{4}$$

is the peak potential value; e and m are the charge and mass of an electron; λ is the laser wavelength; and c is the speed of light in vacuum. The potential produces a gradient force

$$\boldsymbol{F}(x,y,t) = -\nabla U(x,y,t), \tag{5}$$

with x- and y-axis components

$$F_x(x,y,t) = \frac{2U_0(x-l)}{w^2}u(x,y,t),$$
$$F_y(x,y,t) = \frac{2U_0(y-d)}{w^2}u(x,y,t). \tag{6}$$

The F_x force component modulates the electron velocity, and the F_y component deflects the electrons from the initial beam axis. The combined action of these forces may lead to both focusing and collimation of that part of the electron beam which is in the region of the ponderomotive potential during the laser pulse.

In the examples below, the ponderomotive potential is created by a pulsed laser beam with a wavelength $\lambda = 800$ nm and pulse duration $\tau_{las} = 50$ fs. A 100-eV electron beam emerges from a region of cross-sectional size $\delta d = 0.5$ μm and propagates within an angle $2\theta = 1^\circ$. The initial electron pulse duration, τ_e, is taken to be several times the laser pulse duration, τ_{las}. The peak laser beam intensity, I_0, is $10^{14} - 10^{15}$ W cm^{-2}, the level at which the ponderomotive potential maximum, U_0, is 10 – 100 eV.

As the first example, consider the use of the ponderomotive potential created by a Gaussian laser beam. Figure 3 illustrates the deflecting and focusing action of the gradient force of a Gaussian beam on an electron beam with the above parameters at an intensity $I_0 = 2\times 10^{15}$ W cm^{-2}, a beam radius in the caustic $w = 3$ μm and beam centre coordinates $l = 100$ μm and $d = 3.5$ μm. The trajectories were obtained by numerically solving the equations of electron motion under the action of the force components (6). The dashed line represents the 1/e laser beam cross section, corresponding to a radius $w = 3$ μm. Note that the laser beam in Fig. 3 has an elliptical cross section because the x and y axes differ in scale. The electron beam deflection in this example is $\sim 5^\circ$.

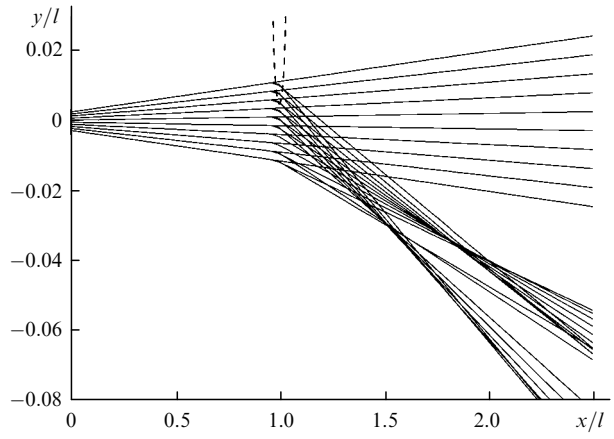

Figure 3. Electron beam deflection and focusing by an ultrashort Gaussian laser beam.

It should be emphasised that the pulsed ponderomotive potential, of course, deflects only that part of the electron beam which is in the region of the laser beam during the rather short optical pulse. Accordingly, a major part of the electron beam propagates unaffected by the laser pulse, and only a small part of the beam deflects. In effect, the fraction of deflected electrons is determined by the electron and laser pulse repetition rates and the relationship between the electron and laser pulse durations. If, in the simplest case, the repetition rate of laser pulses coincides with that of electron pulses, the fraction of deflected electrons can be estimated as $\beta = \tau_{las}/\tau_e$.

Figure 4 illustrates the deflecting and collimating action of the gradient force of a Gaussian beam on an electron beam. The electron beam is exposed to laser pulses of intensity $I_0 = 9\times 10^{14}$ W cm^{-2} at a laser beam radius in the caustic $w = 3$ μm and beam centre coordinates $l = 100$ μm

and $d = 2.9$ μm. The dashed line represents the laser beam cross section corresponding to a radius $w = 3$ μm. The electron beam deflection here is also $\sim 5^\circ$.

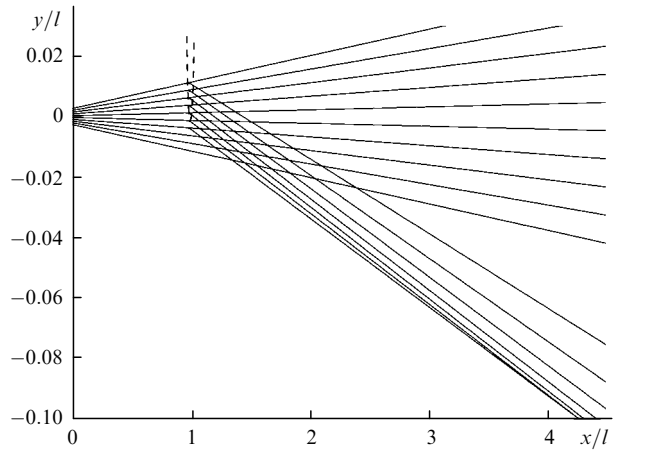

Figure 4. Electron beam deflection and collimation by an ultrashort Gaussian laser beam.

In the above examples, the deflected beam can be separated from the parent beam by appropriate apertures.

3. Electron beam focusing and collimation by a hollow laser beam

A pulsed hollow laser beam (Fig. 1b) may act on an electron beam as a focusing lens. Let a hollow beam have an intensity distribution of form (1) with the normalised envelope

$$u(x,y,t) = \frac{(x-l)^2 + y^2}{w^2}$$

$$\times \exp\left[-\frac{(x-l)^2 + y^2 - w^2}{w^2}\right] \exp\left[-\left(\frac{t-t_0}{\tau_{las}}\right)^2\right]. \quad (7)$$

Envelope (7) has a maximum value of unity at $t = t_0$ and a radial displacement from the beam axis $r = [(x-l)^2 + y^2]^{1/2} = w$. Accordingly, the transverse laser beam profile has the highest intensity, I_0, along a circle of radius w. With this intensity profile, the components of the gradient force (5) are

$$F_x(x,y,t) = \frac{2U_0(x-l)}{w^2}\frac{(x-l)^2 + y^2 - w^2}{w^2}u(x,y,t), \quad (8)$$

$$F_y(x,y,t) = \frac{2U_0 y}{w^2}\frac{(x-l)^2 + y^2 - w^2}{w^2}u(x,y,t). \quad (9)$$

A hollow laser beam can be used to focus and collimate an electron beam. Figure 5 illustrates electron beam focusing by the gradient force of a hollow laser beam at the above parameters of the laser and electron beams, a peak intensity $I_0 = 4 \times 10^{14}$ W cm^{-2}, beam radius in the caustic $w = 4$ μm, and beam centre coordinate $l = 100$ μm. The dotted line in Fig. 5 represents the cross section of the laser beam of radius $w = 4$ μm at the maximum in the transverse intensity profile. In this example, the ponderomotive potential focuses

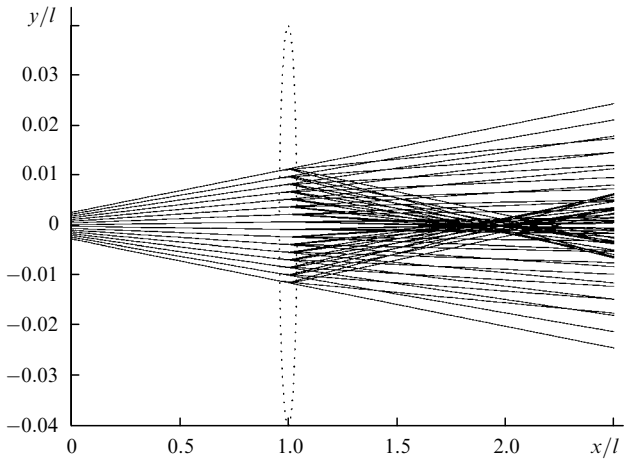

Figure 5. Pulsed focusing of an electron beam by a hollow laser beam.

the electron beam in the hollow region of the laser beam during the laser pulse.

Figure 6 illustrates the collimating effect of the gradient force on an electron beam. Here, the peak intensity of the hollow laser beam is $I_0 = 1.6 \times 10^{14}$ W cm^{-2}, the beam radius in the caustic $w = 4$ μm and beam centre coordinate $l = 100$ μm. The other parameters of the laser and electron beams are the same as above. The dotted line in Fig. 6 represents the cross section of the laser beam of radius $w = 4$ μm at the maximum in the intensity profile. Note once more that the beams in Figs 5 and 6 have an elliptical cross section because the x and y axes differ in scale.

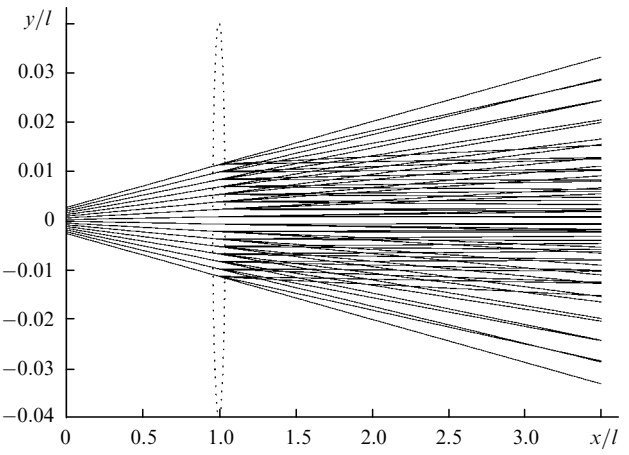

Figure 6. Pulsed collimation of an electron beam by a hollow laser beam.

In these two examples, the focused or deflected electron beam can also be separated by appropriate apertures.

4. Conclusions

The above analysis shows that a femtosecond ponderomotive optical potential can effectively isolate a femtosecond electron bunch from the parent, longer electron pulse. This can be achieved by deflecting, focusing and/or collimating electron bunches. At a relatively low initial electron beam energy (~ 100 eV) and a laser beam

diameter of ~ 10 μm, a laser beam intensity from $\sim 10^{14}$ to 10^{15} W cm^{-2} is sufficient for effectively controlling the parameters of the electron beam. The focal length of such a laser lens is ~ 100 μm.

It should also be emphasised that, as shown in the above analysis, illustrated by Figs 3–6, laser steering is most effective in the case of narrow electron beams, i.e. beams precollimated by apertures. When a narrow electron beam is used, most of the electrons can traverse the region of a sufficiently smooth ponderomotive potential and, accordingly, experience a sufficiently regular deflection, focusing and/or collimation.

Acknowledgements. The author is grateful to S.A. Aseev and B.N. Mironov for useful discussions. This work was supported in part by the Russian Foundation for Basic Research (Grant No. 07-02-00748-a).

References

1. Zawadzka J., Jaroszynski D.A., Carey J.J., Wynne K. *Nucl. Instrum. Methods Phys. Res., Sect A,* **445**, 324 (2000).
2. Niikura H., Legare F., Hasbani R., Bandrauk A.D., Ivanov M.Yu., Villeneuve D.M., Corkum P.B. *Nature*, **417**, 917 (2002).
3. Irvine S.E., Dechant A., Elezzabi A.Y. *Phys. Rev. Lett.*, **93**, 184801 (2004).
4. Hommelhoff P., Sortais Y., Aghajani-Talesh A., Kasevich M.A. *Phys. Rev. Lett.*, **96**, 077401 (2006).
5. Mironov B.N., Aseev S.A., Chekalin S.V., Letokhov V.S. *Pis'ma Zh. Eksp. Teor. Fiz.*, **83**, 435 (2006).
6. Mironov B.N., Aseev S.A., Minogin V.G., Chekalin S.V. *Zh. Eksp. Teor. Fiz.*, **133**, 1155 (2008).
7. Balykin V.I., Subbotin M.V., Letokhov V.S. *Opt. Commun.,* **129**, 177 (1996).
8. Minogin V.G., Fedorov M.V., Letokhov V.S. *Opt. Commun.,* **140**, 250 (1997).
9. Hebeisen C.T., Ernstorfer R., Harb M., Dartigalongue T., Jordan R.E., Miller R.J.D. *Opt. Lett.*, **31**, 3517 (2006).
10. Baum P., Zewail A. *Chem. Phys. Lett.*, **462**, 14 (2008).
11. Mao S.S., Quere F., Guizard S., Mao X., Russo R.E., Petite G., Martin P. *Appl. Phys. A*, **79**, 1695 (2004).
12. Tien A.C., Baskus S., Kapteyn H., Murnane M., Mourou G. *Phys. Rev. Lett.,* **82**, 3883 (1999).